RT-SIL Performance Analysis of Synchrophasor-and-Active Load-Based Power System Damping Controllers

G.M. Jonsdottir*, M.S. Almas*, M. Baudette*, M.P. Palsson¶, L. Vanfretti*†

*Electric Power Systems Department, KTH-Royal Institute of Technology, Stockholm, Sweden
Email: {gmjon, msalmas, baudette, luigiv}@kth.se
†R&D Department, Statnett SF, Oslo, Norway, Email: luigi.vanfretti@statnett.no
¶System Planning Department, Landsnet, Reykjavik, Iceland, Email: magnip@landsnet.is

Abstract—The Icelandic power network has transmission constraints that often lead to inter-area oscillations. Although conventional stabilization methods have been applied successfully in the past, there is potential to exploit large industrial loads to enhance system stability during stringent operation conditions. This paper analyzes the performance of two damping controllers. The controllers can use both synchrophasor signals and local measurements as their inputs. Damping is achieved by load modulation generated by a phasor-based oscillation signal. Real-Time Software-in-the-Loop testing is performed using Opal-RT's eMEGAsim Real-Time Simulator to derive hardware and computational requirements of a hardware prototype that will be implemented in the future.

Index Terms—Active Load Control, Power Oscillation Damping, Real-Time Simulation, Opal-RT, SmarTS-Lab.

I. Introduction

Electromechanically induced low frequency inter-area oscillations may appear in a heavily loaded power system where large generation and load centers are separated by a long transmission line. Inter-area oscillations emerge as a group of generators in one area oscillating against a group of generators in another area [1]. The Icelandic power system experiences inter-area oscillations during periods of stressed operation. The $0.64\,\text{Hz}$ inter-area mode is dominant in the north and east of the country where the machines connected to 132kV ring oscillates in anti-phase with the 220kV network. Similary, an $0.8\,\text{Hz}$ inter-area mode is observable in the eastern and western sections of the 132kV network [2].

Electric power systems have traditionally relied on generators and transmission equipment for maintaining system stability. For damping of inter-area oscillations, Power System Stabilizers (PSS) have been widely used [3] and more recently power electronics based Flexible AC Transmission systems (FACTS) have been explored to provide adequate damping to these inter-area oscillations [4]. On the other hand, loads have been used to prevent under-frequency operation or to avoid blackouts. However, there is potential to use loads for stability enhancement during stressed network operation. The use of active load control was discussed already in 1968 [5] but at that time it was not an economical option. In more recent years the importance of giving the load a more active role in stabilizing the system has been identified and there is a renewed interest in load control [6].

In this paper the modified version of 2-area 4-machines Klein-Rogers-Kundur power system test case [7] is modelled in MATLAB/SIMULINK [8] and two different load control algorithms are proposed to provide inter-area oscillation damping. The load controls rely on a phasor based oscillation damping algorithm where the main objective is to separate the oscillatory part of the input signal from the average value signal [9] [10].

The test case model together with developed load control algorithms are executed in Real-Time using Opal-RT's eMEGAsim Real-Time Simulator [11]. This approach of testing the control algorithm is called Real-Time Software-in-the-Loop (RT-SIL) which is a technique used in model-based control design [12]. RT-SIL is verification and validation technique used towards the development of a hardware prototype. Performance analysis of the tests using this approach allow to derive requirements for hardware and computational resources of a prototype to be implemented in the future.

The remainder of this paper is organized as follows. Test system modelling is described in Section II. Two active load control algorithms are presented in Section III. Section IV discusses the Real-Time SIL approach for validating the developed algorithms. RT-SIL simulation results for inter-area oscillation damping are discussed in Section V, and finally, conclusions and future work are outlined in Section VI.

II. Test system modelling

In order to investigate the performance of the developed load control algorithms, 2-area 4-machines Klein-Rogers-Kundur test system [7] was modelled in the MATLAB/SIMULINK environment using the SimPowerSystems (SPS) Toolbox [8] and was executed in real-time using Opal-RT's eMEGAsim Real-Time Simulator [11]. The single line diagram of the test case is shown in Fig. 1. The SPS toolbox is a dedicated tool for power systems modelling and simulation and is compatible with the real-time simulator used in this study.

The test system consists of two symmetrical areas interconnected through two parallel $230\,\text{kV}$ transmission lines of $220\,\text{km}$ length. Each area has two round rotor generators that are identical and are rated $20\,\text{kV}/900\,\text{MVA}$. The nominal power system frequency for the test case models is $50\,\text{Hz}$. The load is split between the two areas in such a way that Area 1 is exporting about $416\,\text{MW}$ to Area 2. In the original model all loads were represented as constant impedances. This system was designed specifically to study electromechanical oscillations in large interconnected power systems [1]. In the
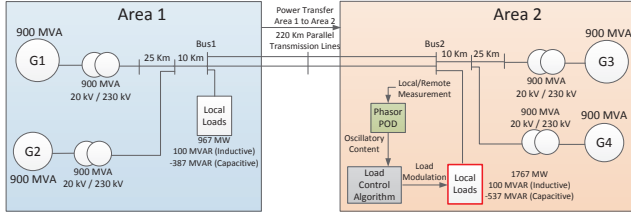
Fig. 1. Single line diagram of the test case power system model

absence of any oscillation damping controller, the test case system is unstable when subjected to either a small or large disturbance and results in an undamped oscillation of $0.64\,Hz$ which can be seen in the tie-line power transfer from Area 1 to Area 2 in Fig. 2.
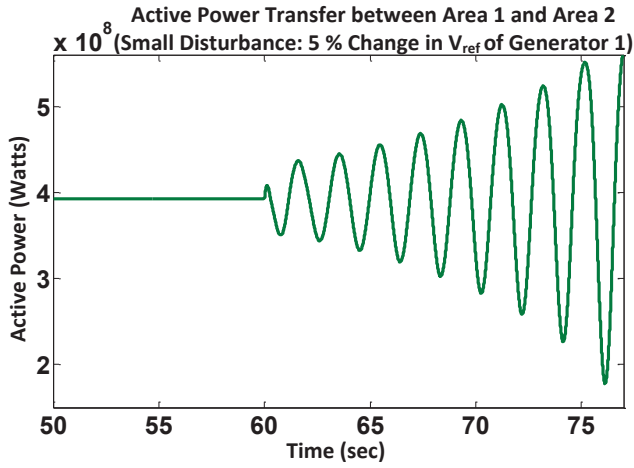

Fig. 2. Active power transfer between Area 1 and Area 2 in absence of power oscillation damping control. A small disturbance is introduced in the test case system at $t = 60\,sec$. An undamped oscillation of $0.64Hz$ can be observed in the measured active power through the tie-line.

In order to implement the active load control algorithm, the load in Area 2 was modified as a three phase dynamic load, the active power of which is controlled by the load control algorithm. In order to analyze the performance of developed active load control algorithms, two disturbances were introduced in the test-case system:

Scenario 1 A small disturbance in the form of 5% positive magnitude step in the reference voltage of Generator 1 applied for 4 cycles at $t = 60\,sec$.

Scenario 2 A large disturbance in the form of three phase to ground fault (4 cycles, i.e. $80\,ms$) at $t = 60\,sec$ in the middle of one of the two $220\,km$ transmission lines connecting together the two areas.

Both these scenarios result in an undamped $0.64\,Hz$ inter-area oscillation. The active load control algorithms were implemented to damp this oscillation, as discussed in the next section.

III. LOAD CONTROLS

A. Algorithm 1

The first algorithm to control the active part of the load is shown in Fig. 3 and is applied to the dynamic load in Area 2 to provide damping for this $0.64\,Hz$ inter-area mode. The approach used for generating command signals for load control is inspired from the phasor based oscillation damping (Phasor-POD) algorithm proposed in [9], see Fig. 3. The Phasor-POD approach separates the oscillatory part from the measured average value of the input signal either by using recursive least square technique or by low pass filtering. In this study, the active power transfer between Area 1 and Area 2 is used as an input signal for the load control algorithm. However, the flexibility of the Phasor-POD algorithm facilitates to utilize any local or remote measurement as an input to the load control algorithm.
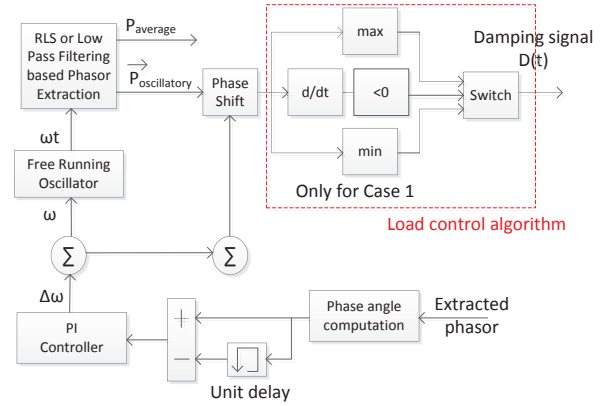

Fig. 3. Active Load Control Algorithm 1

To create the control signal for active load modulation, the derivative of the oscillatory content of active power (input signal) is calculated. During the inter-area oscillations, the active power transfer through the tie-line is greater than the steady-state active power transfer for one half of the oscillatory cycle and is lesser than the steady-state active power transfer in the other half of the oscillatory cycle. When the active power transfer through the line starts increasing, the load control algorithm issues command to the dynamic load in A2 to increase its active power consumption. The inverse is valid when the active power transfer through the tie-line starts decreasing. In order to determine the amount of increase in active power load consumption, the maximum value of the oscillatory signal is found for each cycle. Similarly, the amount of load to be shed is determined by the minimum value of the input oscillatory signal for each cycle.

B. Algorithm 2

The second active load control algorithm developed is almost identical to the one presented above. The only difference is that the dynamic load's active power consumption is

allowed to increase based on the command of the load control algorithm but is blocked when the load control algorithm issues a command for load shedding. This gives additional flexibility to Transmission System Operators (TSOs) where they can avoid load shedding and still achieve adequate inter-area oscillation damping.

IV. Software-in-the-Loop Validation

In order to analyze the performance of the developed active load control algorithms, Real-Time Software-in-the-Loop (RT-SIL) simulation [12] of the test case system was performed using Opal-RT's eMEGAsim Real-Time Simulator. When using the RT-SIL approach, both the controller and the test case are simulated in real-time in the same simulator but using three different computation cores; two for the test system model and a separate one for the load control.

Figure 4 shows the steps that were followed for Real-Time SIL validation. The control signal output of the load control algorithm was fed to one of the digital output of the simulator. This digital output was physically looped back (i.e. hardwired) through one of the I/Os of the simulator. That digital input was configured to modulate the active load consumption of the dynamic load in Area 2. Figure 4 shows some of the necessary steps required for executing the test case model in real-time e.g. model splitting into different subsystems, using vendor specific blocks for communicating between the subsystem, compiling the model and finally executing it in real-time. The test case model together with control algorithms were executed in real-time with a step size of $50\,\mu$sec and by utilizing three cores of real-time simulator.
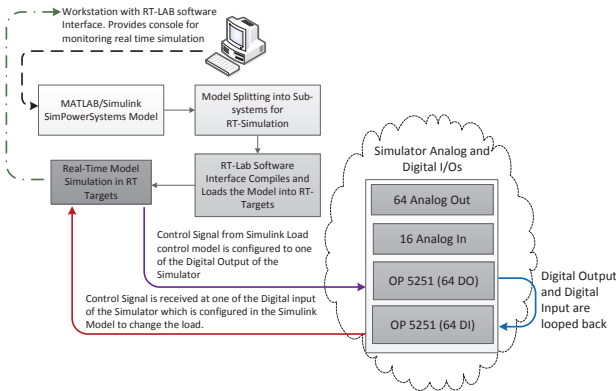

Fig. 4. Steps for Real-Time Software-in-the-Loop (RT-SIL) simulation.

V. Discussion on Simulation results

RT-SIL simulation results are presented in this section for both the test case scenarios, i.e. performance of the developed active load control algorithms for both small and large disturbances.

A. Small Disturbance Analysis

The performance of both the active load control algorithms when the test case system is subjected to a small disturbance is shown in Fig. 5. In the absence of any oscillation damping control, the rotor angle deviation and rotor angle speed starts oscillating with $0.64\,$Hz inter-area oscillation frequency instantaneously after the disturbance is applied at $t = 60\,$sec. At about $t = 75\,$sec, the generator 1 (Area 1) loses synchronism and the system collapses. The same is valid from the plot of power transfer between Area 1 and Area 2, where after $t = 15\,$sec of introduction of fault, the power oscillation increases to about $100\,$MW. However in the presence of the active load control algorithm, the inter-area oscillations are damped within $t = 8\,$sec. Active load control algorithm 1 provides quicker damping as compared to algorithm 2. This was expected as algorithm 1 provides damping by both increasing the active load consumption and shedding it off. Figure 5 plot d, shows the active power modulation of dynamic load in Area 2. The red trace shows the load variation due to active load control algorithm 1, where the load is both increased and shed off to damp the inter-area oscillations. The blue trace shows the load modulation due to active load control algorithm 2, where load shed off is blocked and only the increase in load is used to damp this $0.64\,$Hz inter-area oscillation.

B. Large Disturbance Analysis

When the test case system is subjected to a large disturbance, the resultant first swing causes the active load control algorithm to inject/consume a lot of active power thus causing the system to collapse. A remedial strategy was adopted by blocking the active load control algorithm for $t = 2.5\,$sec after the introduction of large disturbance. This resulted in a fair performance of both the active load control algorithms to damp inter-area oscillations which can be seen in Fig. 6.

Similar to the earlier scenario, the system is unstable in the absence of any oscillation damping control once the large disturbance is applied at $t = 60\,$sec. The plot of power transfer between Area 1 and Area 2 shows a power oscillation of about $200\,$MW after $t = 15\,$sec of introduction of fault. Once the active load control algorithm is enabled, the inter-area oscillations are damped within $t = 10\,$sec. As justified for the earlier test case scenario, active load control algorithm 1 provides quicker damping as compared to algorithm 2. Figure 6 plot d, shows the active power modulation of dynamic load in Area 2 as driven by both active load control algorithms. The red trace shows the load variation due to active load algorithm 1, where the load is both increased and shed off to damp the inter-area oscillations. The blue trace shows the load modulation due to active load algorithm 2, where load shed off is blocked and only the increase in load is used to damp this $0.64\,$Hz inter-area oscillation.

C. Real-Time Simulator's Resource Utilization

All the test scenarios were executed in real-time using three cores of Opal-RT's eMEGAsim Real-Time Simulator with a

Scenario 1: Small disturbance (5 % Change in V_ref of Generator 1)
Rotor Angle Deviation of Generator 1

Scenario 1: Small disturbance (5 % Change in V_ref of Generator 1)
Rotor Speed of Generator 1

Scenario 1: Small disturbance (5 % Change in V_ref of Generator 1)
Power Transfer Between Area 1 and Area 2

Scenario 1: Small disturbance (5 % Change in V_ref of Generator 1)
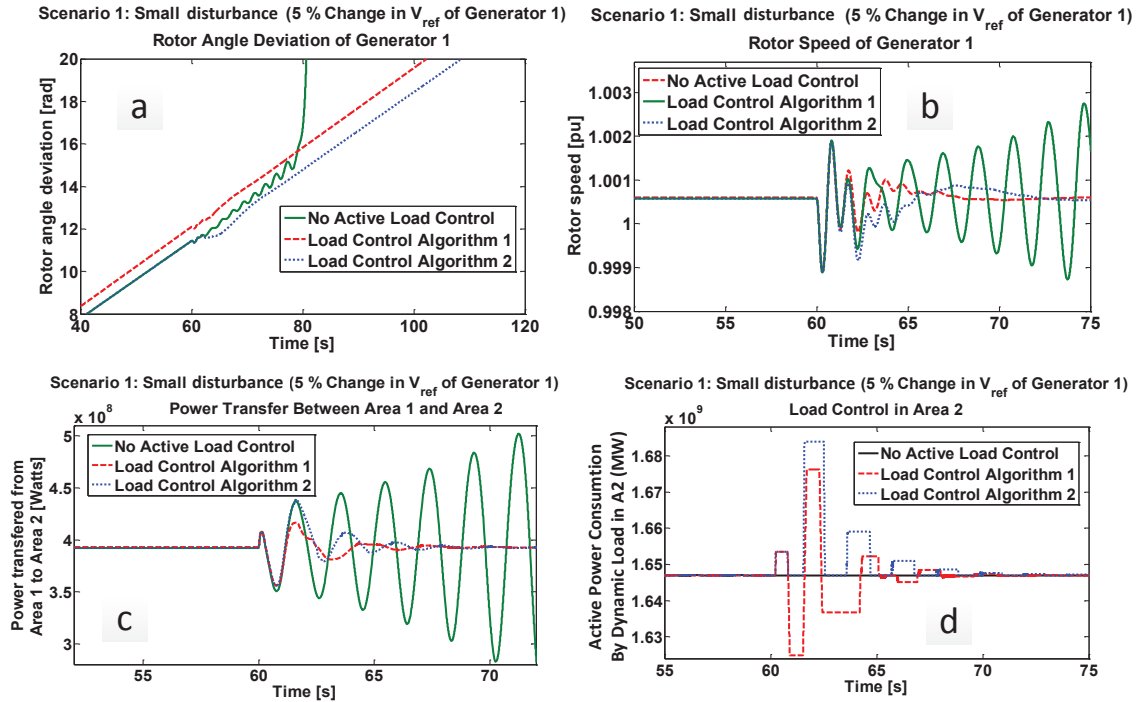Load Control in Area 2

Fig. 5. Response of the test case system when subjected to small disturbance. Plot (a) shows the rotor angle deviation and plot (b) shows the rotor speed of Generator 1. The active power transfer through the tie-line is shown in plot (c). Plot (d) shows the load variation of the dynamic load in Area 2 to provide inter-area oscillation damping. Both the active load control algorithms provide adequate damping to the 0.64 Hz inter-area oscillationn
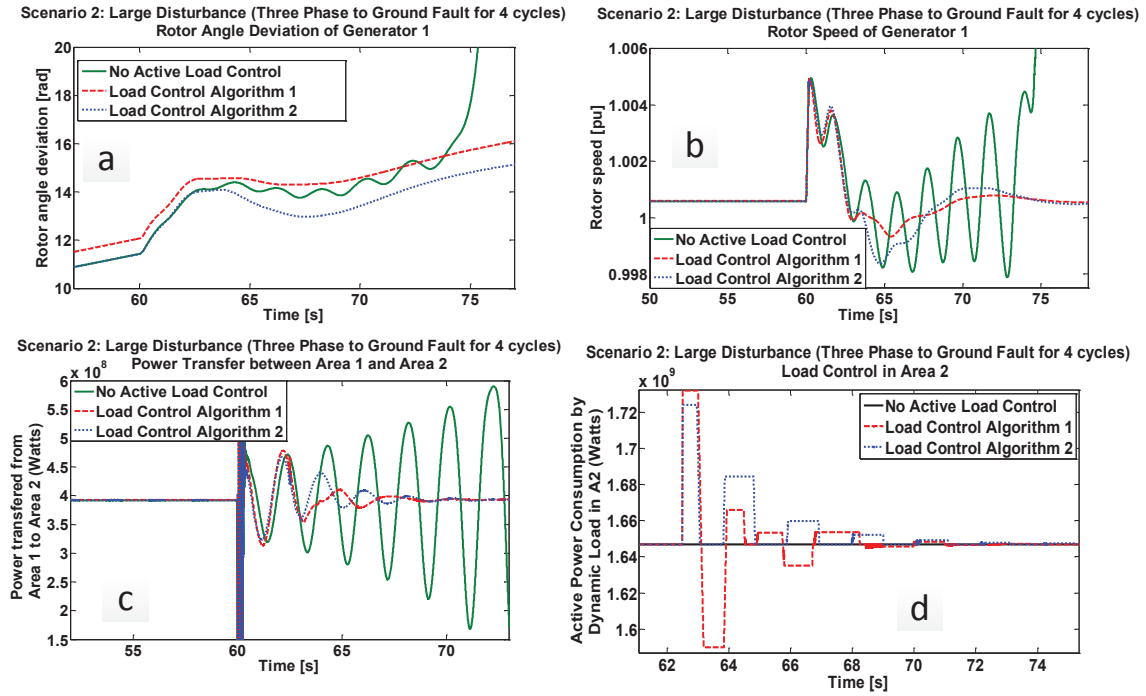
Scenario 2: Large Disturbance (Three Phase to Ground Fault for 4 cycles)
Rotor Angle Deviation of Generator 1

Scenario 2: Large Disturbance (Three Phase to Ground Fault for 4 cycles)
Rotor Speed of Generator 1

Scenario 2: Large Disturbance (Three Phase to Ground Fault for 4 cycles)
Power Transfer between Area 1 and Area 2

Scenario 2: Large Disturbance (Three Phase to Ground Fault for 4 cycles)
Load Control in Area 2

Fig. 6. Response of the test case system when subjected to large disturbance. Plot (a) shows the rotor angle deviation and plot (b) shows the rotor speed of Generator 1. The active power transfer through the tie-line is shown in plot (c). Plot (d) shows the load variation of the dynamic load in Area 2 to provide inter-area oscillation damping. Both the active load control algorithms provide adequate damping to the 0.64 Hz inter-area oscillation

discrete step size of $50\,\mu$sec. Figure 7 shows that the real-time computation time is around $10\,\mu$sec which is well below $50\,\mu$sec step size and thus no over-runs were detected for all the test cases.

For real-time execution, the mathematical model was separated such that two cores of RTS were used for two areas of Kundur Power System and one core was dedicated for load control algorithm. As no over-runs were detected (see Fig. 7), it is justified that the load control algorithm can be implemented in an embedded controller (e.g. National Instrument's based NI-cRIO) with a similar computation capability as of a single core of RTS which in this case is a standard i686 architecture with a CPU speed of 3466 MHz.
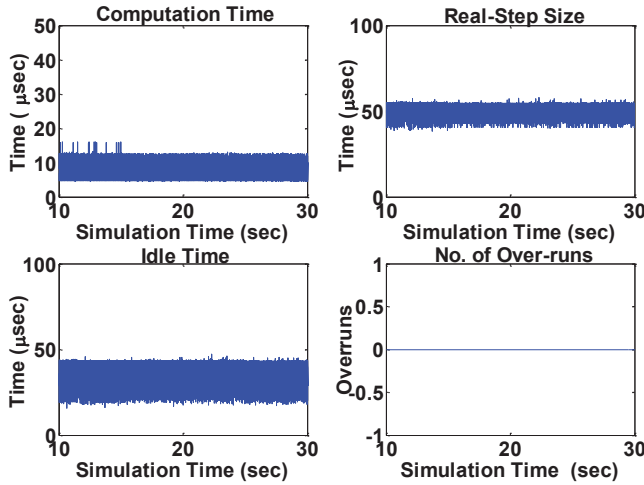

Fig. 7. Real-Time Simulator's resource utilization for the RT-SIL simulation of the test case. The plot (a) shows that the real-time computation time for the test case simulation is around 10μsec with no over-runs detected.

VI. Conclusion

This article presented a performance analysis of two active load control algorithms for providing inter-area oscillations using Real-Time Software-in-the-Loop (RT-SIL). The control algorithms utilize the phasor oscillation damping concept to extract the oscillatory content from the input measurement signal. Active load control algorithm 1 provides damping by both increasing and shedding off the load while algorithm 2 utilize only an increase in active load consumption to serve the same function. Algorithm 1 provides quicker oscillation damping while Algorithm 2 best suits to the Transmission System Operators (TSOs) where load shedding is undesirable to perform oscillation damping.

Future work will be focused on developing a prototype hardware of the developed active load control algorithms based on National-Instrument's Compact Reconfigurable I/O Controllers (cRIOs). In addition, the flexibility of the active load control algorithm will be analyzed by providing both local and *real* Phasor Measurement Units (PMUs)-based remote signals to them to adapt these algorithms to dynamically select

the most appropriate measurement from the dataset as an input to the controller to provide oscillation damping.

References

[1] M. Klein , G. Rogers and P. Kundur "A fundamental study of inter-area oscillations in power systems", IEEE Trans. Power Syst., vol. 6, no. 3, pp.914 -921 1991 .

[2] D. Wilson, K. Hay, P. McNabb, et. al., "Identifying sources of damping issues in the Icelandic power system", Power System Computation Conference (PSCC), Glasgow, Scotland, July 14-18, 2008.

[3] IEEE, "Tutorial Course on Power System Stabilization via Excitation Control", IEEE PES General Meeting, Tampa, Florida, June 2007.

[4] K. Uhlen, L. Vanfretti, M.M. de Oliveira, A. B. Leirbukt, V. H. Aarstrand, and J.O. Gjerde, "Wide-Area Power Oscillation Damper Implementation and Testing in the Norwegian Transmission Network," IEEE PES General Meeting 2012, San Diego, CA, USA.

[5] R. H. Park, "Improved reliability of bulk power supply by fast load control", in Proceedings of the 1968, American Power conference, 1968, pp. 445-457.

[6] I. Kamwa, R. Grondin, et. al., "Large-scale Active-load Modulation for Angle Stability Improvement", IEEE Trans. on Power Systems, Vol. 14, Issue 2, pp. 582-590, May 1999 .

[7] P. Kundur, *Power system stability and control*, McGraw-Hill Inc., 1994.

[8] The MathWorks, "SimPowerSystems User Guide", available online.

[9] L. Angquist and C. Gama, "Damping algorithm based on phasor estimation", IEEE PES Winter Meeting, 2001, Vol. 3, pp. 1160-1165.

[10] M. S. Almas and L. Vanfretti, "Implementation of Conventional and Phasor Based Power System Stabilizing Controls for Real-Time Simulation", IEEE IECON, Dallas, USA, Oct 29-Nov 01, 2014.

[11] Opal-RT, "eMEGAsim PowerGrid Real-Time Digital Hardware in the Loop Simulator," available on-line: http://www.opal-rt.com/ .

[12] C. Bonivento, M. Cacciari, A. Paoli, and M. Sartini, "Rapid Prototyping of Automated Manufacturing Systems by Software-in-the-Loop Simulation", Chinese Control and Decision Conference (CCDC), Mianyang, China, May 2011.